

# Creep and stress-relaxation in ultra-high modulus linear polyethylene

M. A. WILDING,\* I. M. WARD

*Department of Physics, University of Leeds, Leeds, UK*

It has been shown that the creep and stress-relaxation behaviour of oriented linear polyethylene can be satisfactorily described by a model where two thermally activated processes are acting in parallel. The creep behaviour of an oriented sample which does not reach a constant strain-rate can be described by the addition of a further plastic flow term where the viscosity increases linearly with increasing plastic strain.

## 1. Introduction

In a number of recent publications from this laboratory [1-3] the plastic flow creep behaviour of ultra-high modulus linear polyethylene (LPE) has been described in considerable detail. Particular attention was paid to the effects of orientation and structure, and a wide range of materials was examined including various molecular weight homopolymers, a copolymer and an irradiation cross-linked homopolymer.

The main conclusion of this previous work is that the irrecoverable, or plastic flow, creep, can be described very well by a system consisting of two stress-dependent thermally-activated rate processes acting in parallel [4-6]. The major value of this model is that it may provide an insight into the physical mechanisms responsible for creep. For example, it has been proposed that the two activated processes correspond to deformation mechanisms associated with the molecular network and the crystalline regions, respectively. It appears from observation of how the creep parameters vary over the range of samples used, that the major contribution to the structure-dependence of creep arises from the network process. The crystalline process is not influenced by changing the gross structure, although it is sensitive to the degree of stretch.

The validity of the two-process model is, however, dependent on its ability to provide a comprehensive description of the time-dependent behaviour. The first aim of the present paper is

to examine the application of a modified version of the two-process model to the viscoelastic creep behaviour. The modification was necessitated by the fact that viscoelastic creep occurs in essentially non-equilibrium conditions, where the unmodified two-process model gives a very complex analysis. As will be seen, the modification to be presented does not reduce the significance of the results obtained. Indeed, it is the view of the authors that were the two-process model to be rigorously analysed, it would fit the data even more satisfactorily than was found for the modified version. This fitting procedure permits determination of the spring constants, which cannot be evaluated from a study of steady state plastic creep alone. The two-process model can then be further tested by applying it to stress-relaxation. As will be shown, the results are extremely encouraging, and lead us to the opinion that the model has general validity for relaxation and time-dependent phenomena in ultra-high modulus LPE.

Finally, there is a discussion of the strain-hardening which occurs during creep of the high molecular weight homopolymer at low draw. This is related in general terms to the evaluation of the molecular network during deformation.

## 2. Experimental details

### 2.1. Preparation of samples

The samples used in this study were prepared by melt-spinning at 210°C and quenching in glycerol at 120°C. The resulting monofilament was subse-

\*Present address: Department of Textiles, UMIST, P.O. Box 88, Manchester M60 1QD, UK.

TABLE I Details of samples used

Polymer grade*	$\bar{M}_n$	$\bar{M}_w$	Draw ratio
Rigidex 50	6 180	101 450	20
HO20-54P	33 000	312 000	10
			20

\*BP Chemicals International Ltd.

quently drawn through a glycerol bath at 110°C to give a final filament diameter of approximately 0.1 mm. Details of the method of preparation have been given elsewhere [1, 2]. Two homopolymer grades of LPE were used, and these had the characteristics shown in Table I.

### 2.2. Creep measurements

Creep strain as a function of time was determined using a standard dead-loading creep apparatus in which extension was measured by grip displacement. The very long gauge length (10 cm) ensured that no significant end-effects were present [1]. The sample for testing passed through a copper tube surrounded by a thermostatically-controlled silicone fluid bath, in which the temperature could be maintained constant to within 0.2°C.

The extension was determined by the output of a linear displacement transducer, and the sampling of data was performed according to a logarithmic time sequence controlled by an Acorn "Atom" microcomputer. This latter was equipped with analogue/digital conversion, a real-time clock, and a floppy disk drive. The master program for control of the creep experiment was developed in our laboratory and could handle up to eight inputs. If required, the data could be transferred from the disc to the University's main computer, but for local analysis, plots of creep strain against log (time) and log (creep strain rate) against creep strain could be produced via the microcomputer. A novel feature of the system developed for these

measurements was the fact that timing of a test was automatically established from the moment the load was applied to the specimen. This was achieved by constantly monitoring the output from the transducer prior to loading. The large change in output corresponding to the load being applied, was used to trigger the timing program.

### 2.3. Stress-relaxation measurements

The stress-relaxation data were obtained using a tensile testing device designed and constructed in our laboratories. A fixed grip was attached to a bending beam load cell, and a second grip driven, via an electro-magnetic clutch, by a variable speed gearbox. The sample chamber was thermostatically controlled, and the temperature could be maintained constant to within 0.2°C. The output from the load cell was amplified, and measured using a Servogor chart recorder. For future measurements control by microcomputer would be envisaged.

### 3. Results and discussion

The two-process model is shown schematically in Fig. 1a and consists of two sets of a spring and Eyring dashpot arranged in parallel. This model, which was successfully applied to the long-term plastic flow creep, is difficult to analyse rigorously over the whole time range. In the previous study attention was centred on the equilibrium state in which both springs have attained their maximum extensions, and the stress distribution between the two activated rate processes remains constant. As a consequence the actual values of the spring stiffnesses were undetermined. For a more complete understanding it is desirable to model also the short-term creep behaviour, and to arrive at values for these parameters.

For the model of Fig. 1a the parameters  $[\dot{\epsilon}'_0]_1$  and  $v_1$  are the pre-exponential factor and activation volume, respectively, of process 1. The com-

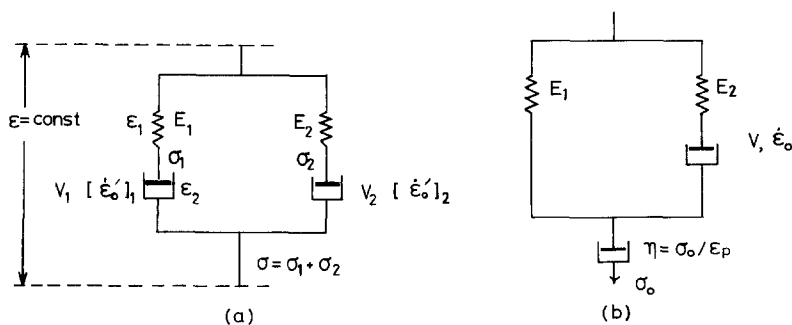


Figure 1 (a) Two-process model under conditions of stress-relaxation. (b) Modified model for viscoelastic creep.

paratively large values obtained for  $v_1 \sim 0.5 \text{ nm}^3$  were considered to be consistent with the identification of this process to the deformation of an oriented molecular network.  $[\dot{\epsilon}'_0]_2$  and  $v_2$  were comparatively unaffected by structural modification, and it was therefore suggested that the activation volume  $v_2 \sim 0.05 \text{ nm}^3$  was consistent with a crystalline deformation mechanism such as the propagation of a Reneker defect through the crystal lattice [7]. The spring stiffnesses  $E_1$  and  $E_2$  are the corresponding moduli of the oriented molecular network and the continuous crystalline fraction, respectively.

At low stress levels and short times the network dashpot is essentially rigid, and it is possible to modify the model slightly without losing its significance to a major extent. Fig. 1b shows this modified system. It is essentially a standard linear solid in series with a dashpot. The latter has been included to deal with the small amount of plastic flow which does occur, even at short times. Because no attempt will be made to model the behaviour over a wide range of stresses with the same parameters this can conveniently be represented by a Newtonian dashpot. The standard linear solid incorporates an activated rate process which corresponds, in general terms, to the crystalline deformation process. It should be emphasized, however, that it is not identical in numerical terms with the same process in the unmodified two-process model where the plastic flow is shared between two dashpots. The springs, on the other hand, do have the same significance as in the two-process model, so that it is possible to use the modified model to evaluate them numerically. Once this has been accomplished the original two-process model may be further tested by applying it to the stress-relaxation behaviour. If this is successful it affords further support to this approach and encourages attempts to ascribe physical significance to the elements of the model.

### 3.1. Analysis of the modified model at a single applied stress level

Consider the strain,  $\epsilon_v$ , developed in the Voigt element in response to an applied creep stress,  $\sigma_0$ . It is assumed that the stress is applied at time  $t=0$ . The instantaneous stresses in the springs  $E_1$  and  $E_2$  are  $\sigma_1$  and  $\sigma_2$  respectively. Then

$$\sigma_0 = \sigma_1 + \sigma_2; \quad \dot{\sigma}_1 = -\dot{\sigma}_2 \quad (1)$$

and

$$\dot{\epsilon}_v = \frac{\dot{\sigma}_2}{E_2} + \dot{\epsilon}_0 \sinh(\sigma_2 v / kT) \quad (2)$$

where  $\dot{\epsilon}_0$  is the pre-exponential factor (which includes the activation energy term) and  $v$  is the activation volume of the Voigt dashpot.

Combining Equations 1 and 2 leads to:

$$\dot{\epsilon}_v = \left( \frac{E_2}{E_1 + E_2} \right) \dot{\epsilon}_0 \sinh \left\{ \frac{(\sigma_0 - \epsilon_v E_1) v}{kT} \right\}. \quad (3)$$

Putting

$$A = \left( \frac{E_2}{E_1 + E_2} \right) \dot{\epsilon}_0$$

and

$$a = \frac{\sigma_0 v}{kT}; \quad b = \frac{E_1 v}{kT}$$

this can be written more simply as:

$$\dot{\epsilon}_v = A \sinh(a - b\epsilon_v).$$

Then

$$\int_{(\epsilon_v)_0}^{(\epsilon_v)t} \frac{d\epsilon_v}{\sinh(a - b\epsilon_v)} = \int_0^t A dt.$$

At  $t=0$  the strain in the Voigt dashpot is zero, so that we have the boundary condition:

$$(\epsilon_v)_0 = \frac{\sigma_0}{E_1 + E_2}.$$

The integration yields:

$$\epsilon_v = \frac{a}{b} + \frac{1}{b} \ln \left\{ \frac{1 - \exp[-b(At + K)]}{1 + \exp[-b(At + K)]} \right\} \quad (5)$$

in which

$$K = -\frac{1}{b} \ln \left( \frac{1 - G}{1 + G} \right)$$

where

$$G = \exp \left[ \frac{b\sigma_0}{(E_1 + E_2)} - a \right].$$

The total strain,  $\epsilon$ , is now obtained by adding the plastic strain developed in the series dashpot. Since this dashpot is subjected to a constant stress,  $\sigma_0$ , it therefore extends at constant rate,  $\dot{\epsilon}_p$ , and

$$\epsilon = \frac{a}{b} + \frac{1}{b} \ln [f(t)] + \dot{\epsilon}_p t \quad (6)$$

where the term in curly brackets in Equation 5 has been replaced by  $f(t)$ .

### 3.2. Results of fitting the modified model to creep

The model described in the previous section was applied to creep data obtained from the Rigidex

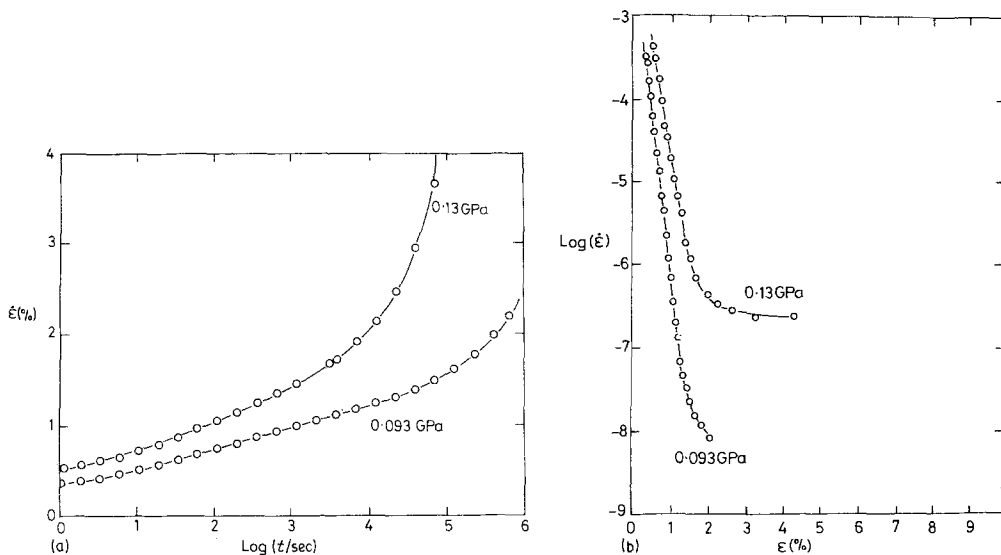


Figure 2 (a) Creep against log (time) curves for Rigidex 50,  $\lambda = 20$  at  $20^\circ\text{C}$ . (b) Log ( $\dot{\epsilon}$ ) against  $\dot{\epsilon}$  plots for Rigidex 50,  $\lambda = 20$  at  $20^\circ\text{C}$ .

50, draw ratio 20 and the HO20, draw ratio 20 samples at  $20^\circ\text{C}$ . Three stress levels were examined for HO20, and two for Rigidex 50. The fitting was carried out using a standard least-squares routine, with the aid of a computer. As was stated earlier, it was not the intention to arrive at the same parameters for all the stress levels, and the fits were performed independently at each stress.

The results are presented both as plots of direct strain against log (time) and also as Sherby–Dorn plots [8]. This follows earlier studies in which Sherby–Dorn plots were found to be a useful means of identifying plastic flow. Fig. 2a

shows the creep curves for the Rigidex 50 sample, whilst Fig. 2b shows the corresponding Sherby–Dorn plots. Figs. 3a and b are the results for the HO20 sample at 0.2 and 0.3 GPa. The full lines in all the plots are the fitted function defined by Equation 6. In qualitative terms the modified model is in excellent agreement with the observed behaviour, even at short times.

The values of the fitted parameters appear in Table II. It is clear from these results that the series dashpot is non-linear, since its viscosity decreases with increasing stress. However, the pre-exponential factor,  $\dot{\epsilon}_0$ , and the activation volume,

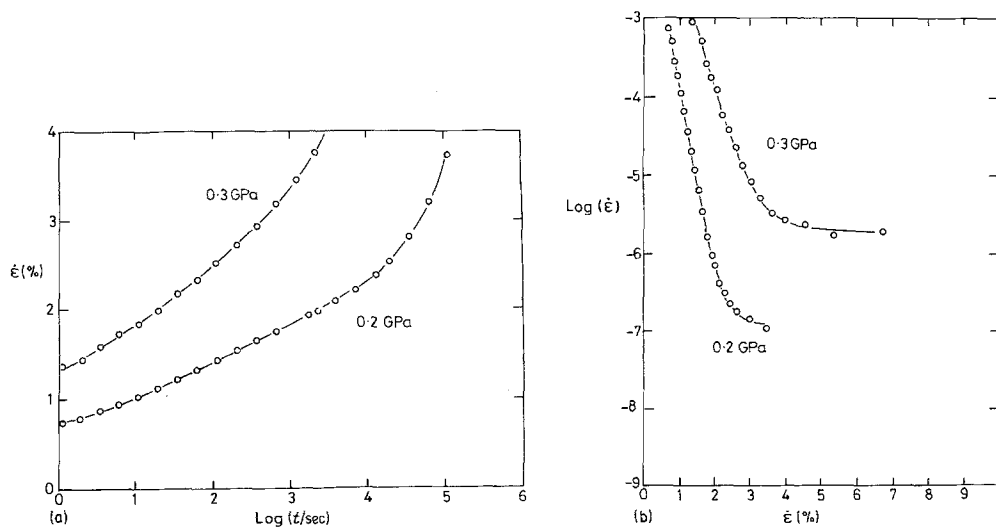


Figure 3 (a) Creep against log (time) curves for HO20,  $\lambda = 20$  at  $20^\circ\text{C}$ . (b) Log ( $\dot{\epsilon}$ ) against  $\dot{\epsilon}$  plots for HO20,  $\lambda = 20$  at  $20^\circ\text{C}$ .

TABLE II Fitted parameters to modified model ( $T = 20^\circ \text{C}$ )

Sample	$E_1$ (GPa)	$E_2$ (GPa)	$v$ (nm <sup>3</sup> )	$\dot{\epsilon}_0$ (sec <sup>-1</sup> )	$\dot{\epsilon}_p$ (sec <sup>-1</sup> )	$\eta (= \sigma_0/\dot{\epsilon}_p)$ (P)
Rigidex 50, $\lambda = 20$ $\sigma_0 = 0.093 \text{ GPa}$	5.6	19.1	0.0665	$4.2 \times 10^{-9}$	$4.1 \times 10^{-8}$	$2.27 \times 10^{15}$
Rigidex 50, $\lambda = 20$ $\sigma_0 = 0.13 \text{ GPa}$	4.89	21	0.0533	$1.4 \times 10^{-9}$	$2.26 \times 10^{-7}$	$5.75 \times 10^{14}$
HO20, $\lambda = 20$ $\sigma_0 = 0.2 \text{ GPa}$	8.28	23.9	0.279	$1.46 \times 10^{-7}$	$1.21 \times 10^{-7}$	$1.65 \times 10^{15}$
HO20, $\lambda = 20$ $\sigma_0 = 0.25 \text{ GPa}$	9.82	26.2	0.201	$2.24 \times 10^{-7}$	$2.33 \times 10^{-7}$	$1.07 \times 10^{15}$
HO20, $\lambda = 20$ $\sigma_0 = 0.3 \text{ GPa}$	6.6	18.1	0.199	$1.07 \times 10^{-7}$	$1.6 \times 10^{-6}$	$1.88 \times 10^{14}$

$v$ , do not appear to be strongly stress-dependent, although we are not necessarily justified in identifying them with the values  $[\dot{\epsilon}'_0]_2$ , and  $v_2$ , obtained from the two-process model (as discussed earlier). The most important observation is that the spring constants are virtually independent of stress. These values should correspond with  $E_1$  and  $E_2$  for the two-process model. Thus, since all the parameters for this model are now known, we are in a strong position to compare the predicted response in stress-relaxation with the observed behaviour.

### 3.3. Analysis of the two-process model for stress-relaxation

For a complete description of the response of the two-process model in stress-relaxation, it is necessary to take account of the finite time over which the initial stress is applied. This arises because relaxation occurs in the two dashpots at different rates during loading. In this connection it might be noted that the model should also describe the stress-strain behaviour at constant strain-rate. However, if the time of loading is short compared with the shortest relaxation time we may make the approximation that the stress distribution at the start of the test is just defined by the spring stiffnesses. This assumption is reasonable for the example to be described.

Fig. 1a shows the two-process model under conditions of stress-relaxation.  $\sigma_1$  and  $\sigma_2$  are the instantaneous stresses in the two arms, whilst  $\sigma$  is the total stress. The total strain is, of course, constant. We define  $\sigma_1(0)$  and  $\sigma_2(0)$  to be the stress components at time  $t = 0$ . From the approximation of a short loading time, we can say:

$$\sigma_1(0) = \frac{\sigma_0 E_1}{E_1 + E_2}$$

$$\sigma_2(0) = \frac{\sigma_0 E_2}{E_1 + E_2}$$

where  $\sigma_0$  is the initial total stress. Because the two processes are in parallel, the stresses are additive, and we need only consider the analysis for one of them. Thus, choosing process 1, we have:

$$\text{total strain} = \epsilon_1 + \epsilon_2 = \text{constant.}$$

i.e.

$$\dot{\epsilon}_1 = -\dot{\epsilon}_2$$

but

$$\dot{\epsilon}_1 = \dot{\sigma}_1/E_1$$

and

$$\dot{\epsilon}_2 = [\dot{\epsilon}'_0]_1 \sinh(\sigma_1 v_1/kT)$$

so

$$\dot{\sigma}_1/E_1 = -[\dot{\epsilon}'_0]_1 \sinh(\sigma_1 v_1/kT)$$

or

$$\frac{d\sigma_1}{\sinh(\sigma_1 v_1/kT)} = -[\dot{\epsilon}'_0]_1 E_1 dt.$$

Thus

$$\int_{\sigma_1(0)}^{\sigma_1} \text{cosech} \frac{\sigma_1 v_1}{kT} d\sigma_1 = -[\dot{\epsilon}'_0]_1 E_1 \int_0^t dt.$$

This integration may be performed in a reasonably straightforward manner, to yield:

$$\sigma_1 = \frac{2kT}{v_1} \operatorname{arctanh} \left\{ \exp \left[ \frac{1}{\gamma_1} (\gamma_1 \delta_1 - t) \right] \right\} \quad (7)$$

in which

$$\gamma_1 = \frac{kT}{[\dot{\epsilon}'_0]_1 E_1 v_1}.$$

$\delta_1$  is the arbitrary constant and is defined by the boundary condition that  $\sigma_1 = \sigma_1(0)$  at  $t = 0$ :

$$\delta_1 = \ln \tanh \left( \frac{v_1 \sigma_1(0)}{2kT} \right).$$

The stress component for the second process,  $\sigma_2$ , is derived in a similar way, and

$$\sigma = \sigma_1 + \sigma_2.$$

TABLE III Parameters used in the fitting of the stress-relaxation data

$E_1$ (GPa)	$E_2$ (GPa)	$v_1$ (nm <sup>3</sup> )	$v_2$ (nm <sup>3</sup> )	$[\dot{\epsilon}'_0]_1$ (sec <sup>-1</sup> )	$[\dot{\epsilon}'_0]_2$ (sec <sup>-1</sup> )
4.89	21	0.456	0.162	$2.4 \times 10^{-13}$	$2.13 \times 10^{-6}$

### 3.4. Comparison of predicted and observed stress-relaxation

In order to test the validity of the two-process model a stress-relaxation test was performed on the Rigidex 50, draw-ratio 20 sample at 20°C over a time scale from 0.2 to 10<sup>6</sup> seconds. The maximum stress applied was 0.27 GPa, this being attained within one or two seconds. The data was then expressed as the fraction of the maximum stress remaining ( $\sigma/\sigma_0$ ) against log (time). The zero of the time scale was taken to be the instant at which the cross-head was arrested. The resulting relaxation curve was then compared with the response function predicted by the two-process model. The parameters used for this appear in Table III. The spring stiffnesses are taken from the fitting procedure for the modified model in creep (Table I), whilst the activation parameters are values obtained in the previous study on plastic flow. The results are shown in Fig. 4. The full line is the model prediction. Bearing in mind the assumptions inherent in the calculation of the predicted curve, and the difficulty in obtaining reliable values for the activation parameters of the low stress process 1, the agreement is good. Although it is not clear from Fig. 4, at very long times the predicted curve would display a second

relaxation during which  $\sigma/\sigma_0$  would fall towards zero. Whether or not this is also true of the actual behaviour cannot be determined without carrying out tests over a very much longer time-scale than is realistically possible. However, the fact that the observed stress does not fall to zero within the experimental time-scale is certainly consistent with the prediction of the two-process model.

### 3.5. Strain-hardening during creep of high molecular weight, low draw material

In a number of creep tests performed on the high molecular weight HO20 sample at draw ratio 10, it was observed that the plots of strain-rate against strain do not show a definite plateau. Nor does the strain-rate fall sharply, as is normally the case in the absence of plastic flow. Rather, the behaviour appeared to be somewhere in between these two extremes, with the strain-rate continuing to fall gradually. In an attempt to study this effect further, the total creep  $\epsilon$  was fitted to the following function:

$$\epsilon = \frac{a}{b} + \frac{1}{b} \ln [f(t)] + Kt^n. \quad (8)$$

This is clearly very similar to Equation 6, but we have allowed a power law dependence of the

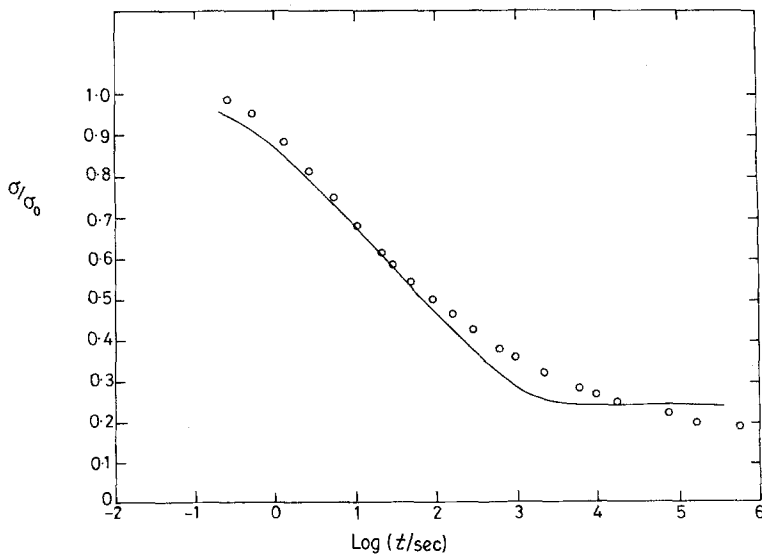


Figure 4 Stress-relaxation data for Rigidex 50,  $\lambda = 20$  at 20°C.

TABLE IV Parameters from fitting equation 7 to HO20,  $\lambda = 10$  creep data ( $T = 20^\circ\text{C}$ )

Sample	$E_1$ (GPa)	$E_2$ (GPa)	$\nu$ (nm <sup>3</sup> )	$\dot{\epsilon}_0$ (sec <sup>-1</sup> )	$K$ (sec <sup>-n</sup> )	$n$
HO20, $\lambda = 10$ $\sigma_0 = 0.125$ GPa	3.9	15.9	0.366	$5.7 \times 10^{-6}$	$3.72 \times 10^{-5}$	0.500
HO20, $\lambda = 10$ $\sigma_0 = 0.15$ GPa	3.7	20	0.303	$1.4 \times 10^{-5}$	$1.1 \times 10^{-4}$	0.505
HO20, $\lambda = 10$ $\sigma_0 = 0.175$ GPa	4.08	15.4	0.271	$2.7 \times 10^{-5}$	$1.5 \times 10^{-4}$	0.515

plastic flow term on time.  $K$  is a constant having the dimensions of  $t^{-n}$ .

The resulting parameters appear in Table IV. The Sherby–Dorn plots are shown in Fig. 5, and it can be seen that there is very good agreement. The most striking feature of the results is that the best value for  $n$  is approximately 0.5. The plastic flow term, denoted by  $\epsilon_p$ , can therefore be written as

$$\epsilon_p = Kt^{1/2}$$

and the strain-rate for a given stress is given by

$$\begin{aligned} (\dot{\epsilon}_p)_\sigma &= \frac{1}{2}Kt^{-1/2} \\ &= \frac{1}{2}K^2 \left( \frac{1}{Kt^{1/2}} \right) \\ &= \frac{K^2}{2\epsilon_p} \end{aligned} \quad (9)$$

i.e., the strain-rate is inversely proportional to the strain.  $K$  will not be constant in general, but will be stress-dependent. If the dashpot is essentially Newtonian then the strain-rate at constant strain must be proportional to the stress, so that:

$$(\dot{\epsilon}_p)_{\epsilon_p} = A\sigma, \quad (10)$$

where  $A$  is a constant independent of stress and strain.

More generally, the strain-rate can be expressed as a function of stress and strain, on the basis of Equations 9 and 10 by putting

$$\dot{\epsilon}_p = A'\sigma/\epsilon_p \quad (11)$$

where  $A'$  is another constant.

Comparison of Equations 9 and 11 gives  $K^2 = 2A'\sigma$ . Equation 11 can be written

$$\sigma = \frac{\epsilon_p \dot{\epsilon}_p}{A'}$$

It follows that

$$\left( \frac{\partial \sigma}{\partial \epsilon_p \dot{\epsilon}_p} \right)_{\dot{\epsilon}_p} = \frac{\dot{\epsilon}_p}{A'} \quad (12)$$

Equation 12 suggests that in a constant strain-rate test the strain-hardening term  $(\partial \sigma / \partial \epsilon_p)_{\dot{\epsilon}_p}$  is non-zero, and in fact must be positive from the definition of  $A'$ . Thus the observation of a  $t^{1/2}$  law in creep is synonymous with positive strain-hardening behaviour.

It also follows that  $(\partial \sigma / \partial \dot{\epsilon}_p)_{\epsilon_p} = \epsilon_p / A'$ , i.e., the viscosity of the series dashpot in Fig. 1b increases with strain.  $(\partial \sigma / \partial \dot{\epsilon}_p)_{\epsilon_p}$  is a term which expresses strain-rate sensitivity. It is known from direct measurements of the flow stress as a function of strain rate [9] that the overall strain-rate sensitivity increases with strain.

#### 4. Conclusions

It has been shown that the total creep behaviour of oriented linear polyethylene, including the

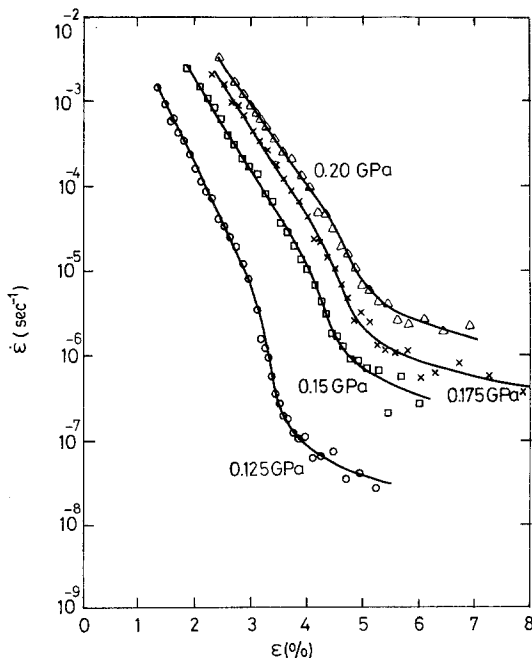


Figure 5 Creep strain-rate against strain for HO20.  $\lambda = 10$  at  $20^\circ\text{C}$ .

initial time-dependent behaviour, can be modelled very satisfactorily by a model in which two thermally activated processes, each in series with an elastic element, are assumed to act in parallel. Furthermore, the stress-relaxation behaviour can also be modelled by this representation, although further studies are required to establish its general validity in this respect.

The creep of one sample, a low draw ratio high molecular weight material, differed in kind from the general creep behaviour of these materials in not reaching a steady flow rate during the tests. A simple model for the two dependent creep of this sample has been proposed. This incorporates a viscosity term which increases linearly with increasing plastic strain.

## References

1. M. A. WILDING and I. M. WARD, *Polymer* 19 (1978) 969.
2. *Idem, ibid.* 22 (1981) 870.
3. M. A. WILDING and I. M. WARD, *Plastics Rubber Proc. Applns* 1 (1981) 167.
4. H. EYRING, *J. Chem. Phys.* 4 (1936) 283.
5. J. A. ROETLING, *Polymer* 6 (1965) 311.
6. C. BAUWENS-CROWET, J. C. BAUWENS and G. HOMÈS, *J. Polym. Sci.* 7 (1969) 735.
7. D. H. RENEKER, *ibid.* 59 (1962) 539.
8. O. D. SHERBY and J. E. DORN, *J. Mech. Phys. Solids* 6 (1956) 145.
9. P. D. COATES and I. M. WARD, *J. Mater. Sci.* 13 (1978) 1957.

*Received 26 May  
and accepted 27 June 1983*